

**Proceedings of the 17th International Symposium on the  
Packaging and Transportation of Radioactive Materials  
PATRAM 2013  
August 18-23, 2013, San Francisco, CA, USA**

**Stability evaluation methodology of the dual purpose metal cask attached to a transfer air pallet  
during long-period seismic motions**

K. Shirai<sup>a</sup>, K. Kanazawa<sup>a</sup>, S. Kawaguchi<sup>b</sup>

<sup>a</sup> Central Research Institute of Electrical Power Industry, 1646 Abiko, Abiko-shi, Chiba-ken 270-1194 Japan

<sup>b</sup> Okumura Corporation, 387 Ohsuna, Tsukuba-shi, Ibaraki-ken 300-2612 Japan

*Corresponding author: K. SHIRAI (shirai@criepi.denken.or.jp)*

**ABSTRACT**

After the nuclear accident occurred on March 11, 2011, strict safety technical requirements on nuclear facilities were issued by Japanese governments to verify countermeasures to assure the safety functions of the facilities even if under severe accident conditions. When the air pallet system is adopted for transfer within the metal cask storage facility site, the metal cask attached to a transfer air pallet may be operated vertically without tie-down system. In order to prevent the damage of the safety functions of the metal cask, it is important to assess the stability of the metal cask attached to a transfer air pallet subjected to strong long-period seismic motions. Considering the similarity law referring the configuration of the metal cask attached to a pallet, 2/5 scale metal cask and transfer pallet models were fabricated and applied for seismic tests on the concrete pad to evaluate its stability under the influence of long-period earthquake motions. Moreover, a rational methodology based on the energy spectrum was proposed and verified as a practical tool for evaluating the occurrence of the overturning when the vertically standing cask without tie-down system.

**INTRODUCTION**

The Tohoku District - off the Pacific Ocean Earthquake with momentum magnitude M9.0 and tsunami attacked the coastal area in Tohoku district on March 11, 2011. After the nuclear accident occurred on March 11, 2011, strict safety technical requirements on nuclear facilities were issued by Japanese governments to verify countermeasures to assure the safety functions of the facilities even if under severe accident conditions. When the air pallet system is adopted for transfer within the metal cask storage facility site, the metal cask attached to a transfer air pallet may be operated vertically without tie-down system. In order to prevent the release of radioactive materials from the containment boundary of the metal cask, it is important to assess the stability of the metal cask attached to a transfer air pallet subjected to strong long-period seismic motions. Considering the similarity law referring the configuration of the metal cask attached to a pallet (such as center of mass, material coefficient of restitution), 2/5 scale metal

cask and transfer pallet models were fabricated and applied for seismic tests on the concrete pad to evaluate its stability under the influence of long-period earthquake motions [1]. As a result, seismic motions with high velocity over 100kine does not always induce the increase of response velocity of the scale model cask because of energy consumption by sliding and local impact deformation of concrete pad at a vicinity of impacted area by the pallet. Moreover, as a method for evaluating the occurrence of the overturning when the vertically standing cask without tie-down system, receives seismic force, attention has been given to the relation with the input energy effective to the cask uplift and the instantaneous input energy in a certain segmented duration time (window width), and the rational energy spectrum (called “Window energy spectrum method”) that contributes to uplift of the cask has been proposed [2]. It is found that the estimated window energy spectrum velocity is fairly in a good agreement with the experimental values and should be a useful tool for practical overturning design of the metal cask attached to a transfer air pallet operated vertically without tie-down system.

### 1. SCALE MODEL

In this chapter, the basic specification of the scale model used in the excitation tests was introduced considering the key parameters (such as gravity center, material coefficient of restitution) which affects to the overturning phenomena of the metal cask attached to a pallet as shown in Fig.1. The weight of the metal cask was 117 tons, and the air pallet was 3.4m x 3.4m square with weight of 21tons. A similarity law was considered in this model to simulate the effect of the gravitational acceleration on the overturning condition of the cask. The similarity law governing the model was summarized as shown in Table 1. The scaling ratios for acceleration and geometry were set to one and two-fifth, respectively and to make equivalent the overturning limit angle (the ratio of the height of the gravity center to the pallet width) the counter weight was added on the top of the scale cask as shown in Fig.2. Moreover, to satisfy the longitudinal stiffness defined by interaction between the air pallet plate and the cask bottom area, the thickness of the pallet plate was decided by the comparison of modal analysis between prototype and scale cask as shown in Fig.3. Table 2 shows the comparison of specifications between the prototype cask and the scale model cask. As a pallet model, Type A (scale model) and Type B (the smaller pallet model) were used to evaluate the influence of the air pallet size on the overturning behavior.

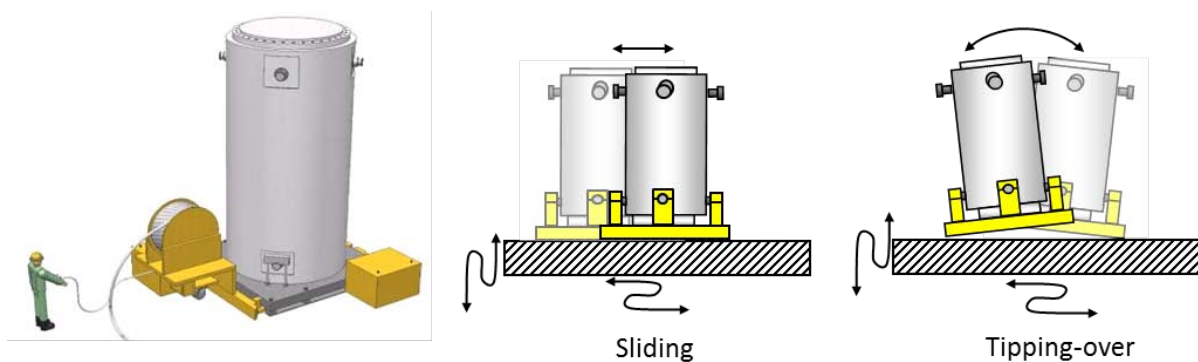


Fig.1 Overturning phenomena of the metal cask attached to a pallet

Table 1. Similarity Law

Parameter	Notation	Dimension	Similarity Ratio	
			General Form*	for N=2/5
Length	L	L	$L_m/L_p = 1/N$	0.4
Time	T	T	$T_m/T_p = 1/N^{1/2}$	0.632
Acceleration	a	$LT^{-2}$	$a_m/a_p = 1$	1
Velocity	V	$LT^{-1}$	$V_m/V_p = 1/N^{1/2}$	0.632
Angle	$\theta$	---	$\theta_m/\theta_p = 1$	1
Mass	M	M	$M_m/M_p = \alpha/N^3$	0.091
Moment of Inertia	I	$ML^2$	$I_m/I_p = M_m L_m^2 / M_p L_p^2 = \alpha/N^5$	0.015
Longitudinal Stiffness	K	$MT^{-2}$	$K_m/K_p = \beta/N$	0.216
Equivalent Cross Section	A	$L^2$	$A_m/A_p = \gamma/N^2$	0.086
Bottom Stress	$\sigma$	$ML^{-1}T^{-2}$	$\sigma_m/\sigma_p = (F_m/A_m)/(F_p/A_p)$	1.0
Longitudinal Force	F	$MLT^{-2}$	$F_m/F_p = (\alpha\beta)^{1/2} \cdot N^{-5/2}$	0.088
Friction Coefficient	$\mu$	---	$\mu_m/\mu_p = 1$	1

Note

\* Suffix p denotes the prototype, and suffix m denotes the scale model

\*\* Considered correction factor :

$\alpha$  (1.43) for mass to make equivalent the overturning limit angle

$\beta$  (0.55) for longitudinal stiffness to make equivalent the longitudinal modal frequency

$\gamma$  (0.57) for cross section of the air pallet column to make equivalent their bottom stress.

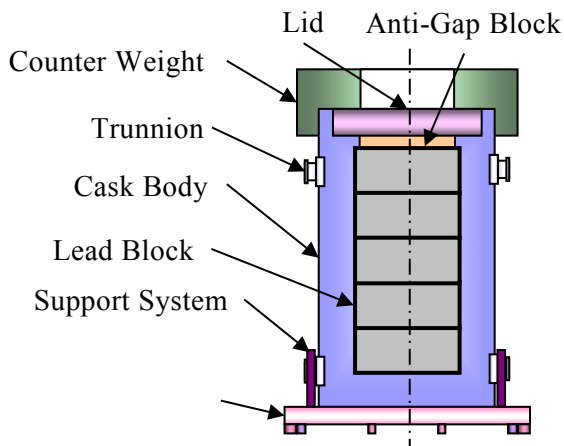


Fig.2 The outline of the scale model

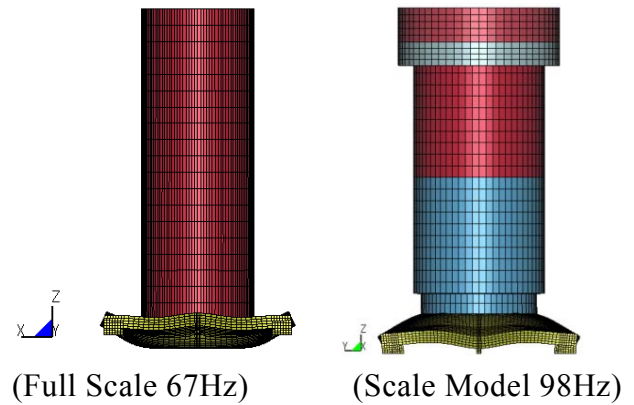


Fig.3 The comparison of the vertical mode

Table 2. Comparison of specification between prototype cask and scale model cask

Part	Unit	Prototype cask	Type A (Scale model)	Type B (Smaller pallet model)
Pallet length	m	3.400	1.360	1.000
Gravity Center Height	m	2.867	1.160	1.210
Mass	ton	138.6	12.465	11.913
Moment of Inertia	$\text{ton} \cdot \text{m}^2$	588.9	6.795	6.007
Overturning Angle	rad	0.535	0.530	0.392

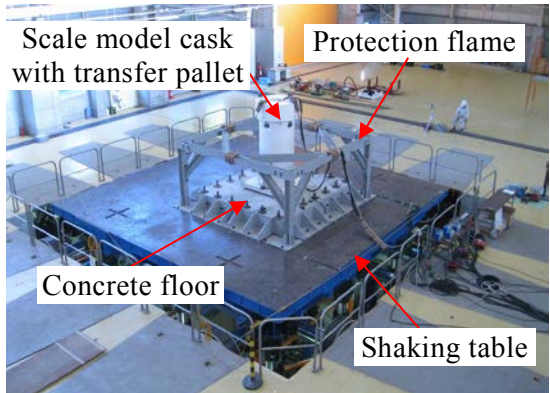
## 2. SHAKING TABLE TEST

### 2.1 Test Apparatus

Shaking table tests were executed using one and three dimensional shaking table test equipment. Table.3. shows the specifications of the test equipment. To clarify the seismic response subjected to the design artificial waves with the very long-period and the size effect of the pallet, one-axis excitation tests were executed. On the other hand, to verify the three dimensional seismic characteristics subjected to the multi-direction input waves with the beyond design amplitude, three-axis large-scale excitation tests were executed. Fig.4 and Fig.5 shows the outline of the scale model cask and concrete floor. A 40cm thick reinforced concrete slab (width 3.18m x length 2.88m) was used as a floor model. Design concrete strength was 30MPa for normal concrete, and D10 reinforced bars made of SD345 were spaced by 100mm pitches. During the seismic excitation test, the angular velocity of the scale model, acceleration of the cask body, pallet and concrete floor, and displacement of the pallet were measured. Data recording sampling frequency were set to 2kHz. The rotational angle was obtained by integrating the angular velocity mathematically.

Table.3 Specifications of the shaking table test equipment

Item	One-axis	Three-axis
Table size	5m×5m	8m×8m
Loading Weight	Nominal 60t Max. 80t	Nominal 100t Max. 30t
Max. Vel.	H ±1.5m/s	H ±2m/s, V ±1m/s
Max. Acc.	H ±1.0G	H ±2.0G, V±1.0G
Max. Disp.	H ±50cm	H ±60cm, V ±30cm
Shaking Frequency	DC ~ 30Hz	DC ~ 50Hz



Scale model cask with transfer pallet

Protection flame

Concrete floor

Shaking table

3-axis large-scale excitation test equipment

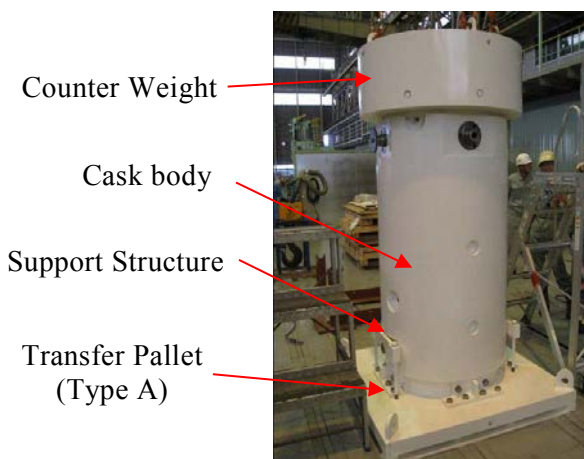
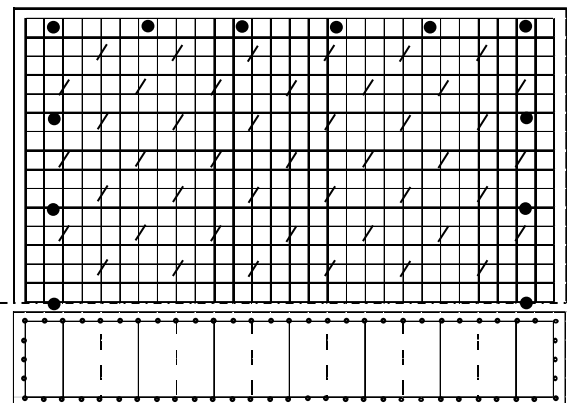


Fig.4 Scale model cask (Type A)



Dimension Width 3,180mm, Length 2,880mm  
Height 400mm  
Reinforcing bars D10@100x100

Fig.5 Outline of the concrete floor

## 2.2 Test Condition

For input of the seismic excitation tests, 6 artificial seismic waves and 17 recorded waves during typical natural earthquake waves (El Centro: Imperial Valley Earthquake, 1940, JMA Kobe: Hyogo-ken Nanbu Earthquake, 1995, etc.) were employed as shown in Table.3. Fig.6 shows examples of the time histories of the artificial waves. Fig.7 and Fig.8 shows the energy response spectrum (dumping factor 10%) of the waves listed in Table.3. In the excitation test, time duration of the input wave was scaled to 0.632 according to a similarity law shown in Table 1 and the acceleration levels were varied according to the test conditions. Test condition includes the cases considering horizontal and vertical motions simultaneously.

Table 3. Specification of input waves

Input Wave	Remarks	Acc. (gal)
AW01	Ss_d #1, Floor Response	1030
AW02	Ss_d #1, Free Base	800
AW03	Ss_i #2, Floor Response	688
AW04	Ss_i #2, Free Base	691
AW05	S <sub>2</sub> #1, Basic Ground Seismic motion	600
AW06	S <sub>2</sub> #2, Magnitude 8.5 Epicenter distance 68 km	407
NW01	1993 Kushirooki, Kushiro	815
NW02	1999 Taiwan, TCU078	439
NW03	1999 Taiwan, TCU129	986
NW04	1994 Sanriku-haruka, Hachinohe	602
NW05	1999 Turkey, Sakarya	399
NW06	2000 Tottori-ken Seibu, Hino, EW	761
NW07	1995 Hyogo-ken Nambu, JMA Kobe, EW	617
NW08	1994 Northledge, Sylmar, ODEG	782
NW09	2001 Geiyo, Yuki, EW	832
NW10	1997 Kagosima-ken Nanseibu, Miyanojo, EW	493
NW11	2003 Miyagi-ken Okinojishin, Onoda, EW	579
NW12	2003 Miyagi-ken Okinojishin, Ojika, NS	1094
NW13	2003 Tokachioki, Hiroo, EW	986
NW14	1979 Coyote Lake, GILROY#6	425
NW15	1983 Coalinga, P.P.-yard	580
NW16	1994 Imperial Valley, El Centro, NS	344
NW17	1952 Kern County, Taft, NS	152

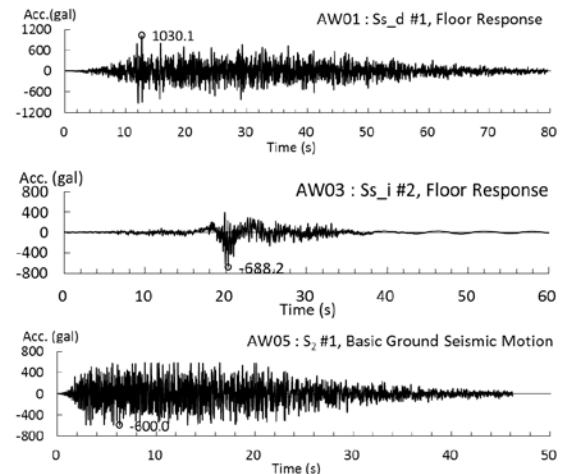


Fig.6 Example of time history for excitation test

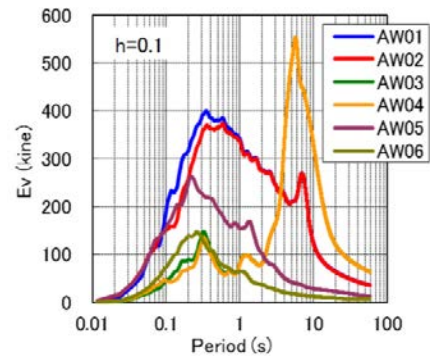


Fig.7 Energy spectrum of artificial waves

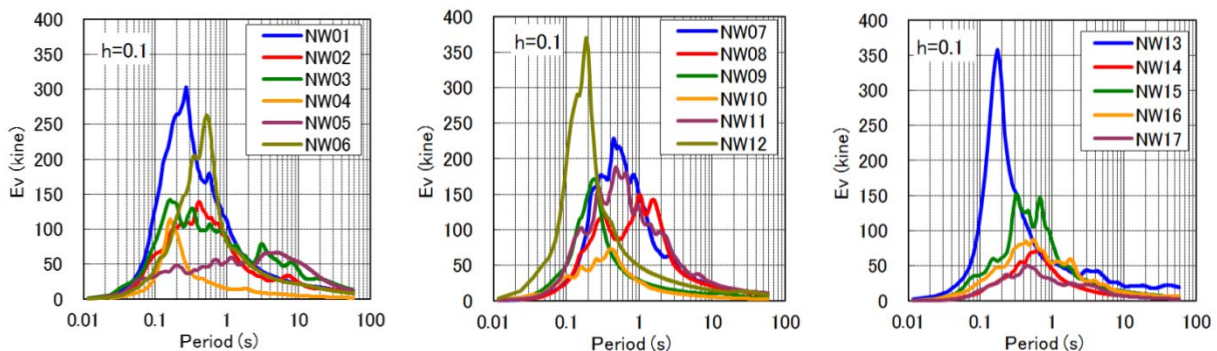


Fig.8 Energy spectrum of natural waves

### 3. TEST RESULTS

#### 3.1 Applicability of the two-dimensional model

To evaluate the applicability of the two-dimensional model to the overturning problem for the metal cask attached to a pallet, the sinusoidal wave tests were executed with type A model and the measured rotational angle values were compared with the theoretical ones for the rigid body as shown in Fig.9. The periodic solution of the non-dimensional response angle  $y$  of the rigid body accelerated by the sinusoidal wave motion  $\ddot{u}=A\cdot\sin\omega t$  ( $A$ : acceleration amplitude,  $\omega$ : angular frequency) can be expressed by Eq. (1). Notation in the equation (1) is designated in Fig.9 [1].

$$y = 1 - \frac{1}{\cosh\pi/2\sigma} - C \frac{PQ - \sqrt{P^2 + 1 - Q^2}}{P^2 + 1} \quad (1)$$

$$n^2 = \frac{Ma}{I_G + Ma^2}, \lambda^2 = n\sqrt{g}$$

$$y = \frac{\theta}{\pi/2 - \alpha}, \sigma = \frac{\omega}{\lambda}, k = \frac{\theta}{g(\pi/2 - \alpha)}, C = \frac{k}{1 + \sigma^2}, P = r\sigma d, Q = \frac{rd^2}{C}, d = \frac{\pi}{2\sigma}, r = \frac{1 - \delta}{1 + \delta}$$

Here,  $\theta$ ,  $g$ ,  $I_G$ ,  $M$ ,  $a$ ,  $\pi/2 - \alpha$ ,  $\sigma$ ,  $k$ ,  $\delta$  are rotational angle, gravitational acceleration, moment of inertia, mass, rotational radius of the gravitational center, overturning angle, non-dimensional frequency, non-dimensional acceleration amplitude, rocking restitution coefficient, respectively. Fig.10 shows the response curve for type A model measured in the sinusoidal excitation tests with the forced amplitude 18mm. As the measured values were good agreement with periodic solutions, the applicability of the two-dimensional model was confirmed.

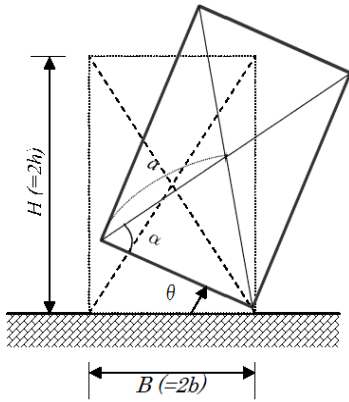


Fig.9 Two-dimensional rectangular rigid body

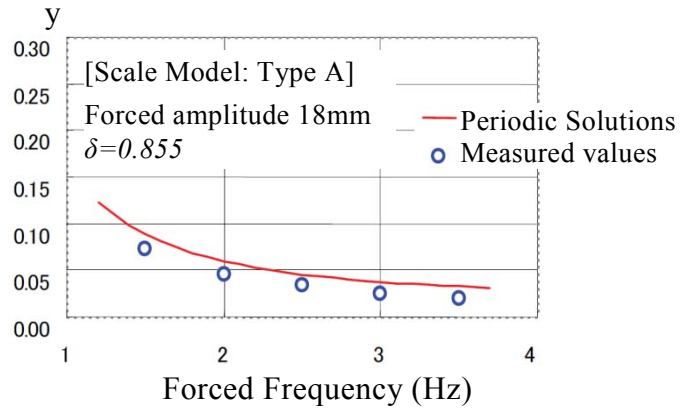


Fig.10 Sinusoidal Response Curve (Type A)

#### 3.2 Window Energy Spectrum

The kinetic equation of the single mass vibration system is express by Eq. (2).

$$m\ddot{y} + c\dot{y} + F(y) = -m\ddot{z} \quad (2)$$

Here,  $y$ ,  $m$ ,  $c$ ,  $F(y)$ ,  $z$  are mass relative displacement, system mass, damping coefficient, restoring force and ground acceleration, respectively. By multiplying each term of Eq. (2) by  $dy=\dot{y}dt$  and integrating during the seismic occurrence duration  $t_0$ , the Eq. (3) can be derived.

The energy spectrums as shown in Fig.7 and Fig.8 were calculated by Eq. (3).

$$m \int_0^{t_0} \dot{y}\ddot{y}dt + c \int_0^{t_0} \dot{y}^2 dt + \int_0^{t_0} F(y)\dot{y}dt = - \int_0^{t_0} m\ddot{z}\dot{y}dt \quad (3)$$

Referring Fig.9, the overturning limit velocity  $V_{Ereq}$  calculated from the critical potential energy of the rigid body can be expressed in Eq. (4).

$$V_{Ereq} = \sqrt{2g/\Delta H} = \sqrt{2ga/(1 - \sin\alpha)} = \sqrt{g(\sqrt{B^2 + H^2} - H)} \quad (4)$$

On the other hand, Akiyama et al. [3, 4] have proposed the equivalent velocity  ${}_{ou}V_{E(a)}$  calculated from input energy to rigid body by Eq. (5). Here,  $V_{E0}$  is the energy spectrum with no damping.

$${}_{ou}V_{E(a)} = \sqrt{\int_{T_0}^{T_1} f(T)\{V_{E0}(T)\}^2 dT}, \quad f(T) = -\frac{2(T - T_1)}{(T_1 - T_0)^2}, \quad T_0 = 0.05\sqrt{a}, \quad T_1 = 0.5\sqrt{a} \quad (5)$$

Finally, criteria for the overturning of the rigid body is defined by Eq. (6).

$${}_{ou}V_{E(a)} < V_{Ereq} \quad (6)$$

In the previous studies, as a methodology to estimate the seismic response of the two-dimensional rigid body, we proposed window energy spectrum  $V_{WES}$  [2] based on energy spectrum originally proposed by Akiyama [3].

Although original energy spectrum  ${}_{ou}V_{E(a)}$  estimates the total energy during the seismic excitation duration  $T_{total}$ ,  $V_{WES}$  is continuously obtained as the instantaneous input energy in a certain segmented duration time (window width:  $T_{window}$ ) as shown in Fig.10. As a  $T_{window}$ , we clarified  $T_1$  gave a good estimation of the uplifting angle by smoothing  $V_{WES}$  with  $T_0$ . Here,  $T_0$  and  $T_1$  are defined in Eq. (5). Fig. 11 shows the  $V_{WES}$  comparing the response energy velocity  $V_{resp}$  (see Eq. (7)) obtained in the excitation test using Type A and Type B. In case of Type B, it is found that as all of the  $V_{WES}$  converted to the uplifting potential energy, the overturning of the model cask was observed just after reaching to the limit velocity  $V_{Ereq}$ .

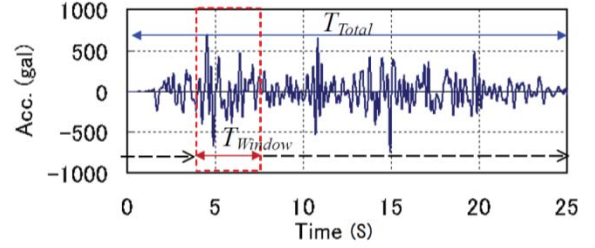
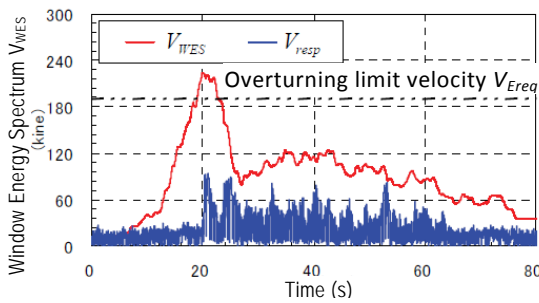
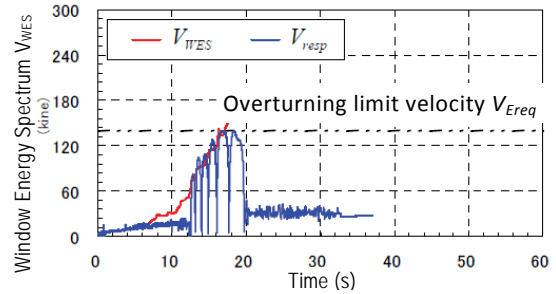


Fig.10  $T_{window}$  for the calculation of  $V_{WES}$

$$V_{resp} = \sqrt{2g\alpha\{\sin(\alpha + \theta) - \sin(\alpha)\}} \quad (7)$$



(Type-A: AW01 1406gal, no over-turning)



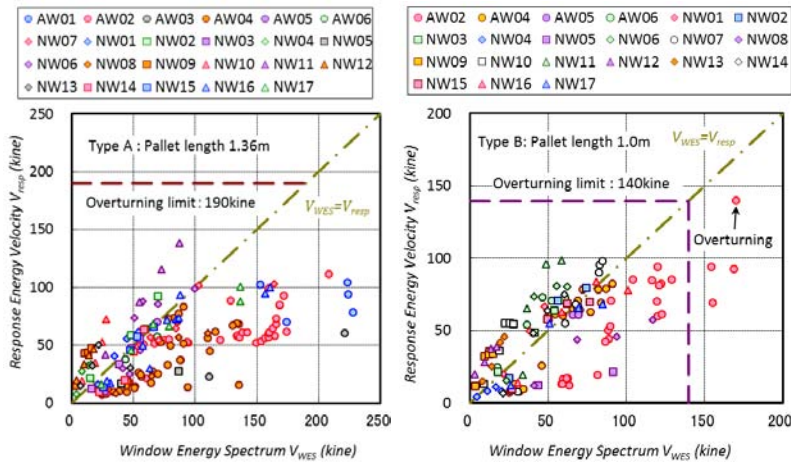
(Type-B: AW01 892gal, over-turning occurred)

Fig. 11  $V_{WES}$  comparing the response energy velocity  $V_{resp}$

### 3.3 Applicability of $V_{WES}$

Fig.12 shows the relationship between  $V_{WES}$  and  $V_{resp}$  obtained in all of the one-axis excitation tests with the artificial and natural seismic waves for Type A and Type B models. As linear increase of  $V_{resp}$  according to the increase of  $V_{WES}$  up to 100kine was observed, it is found that almost of the seismic energy was converted to the uplifting potential energy. However, after exceeding 100kine of  $V_{WES}$ , it seems that the  $V_{resp}$  reaches to the constant level due to the energy

dissipation by sliding on the concrete surface or local damage of the concrete surface in spite of the pallet size. As a result,  $V_{WES}$  is a practical and conservative design parameter to estimate the occurrence of the overturning of the metal cask with the pallet. Fig.13 shows multi-axis excitation tests for Type A. As there was no remarkable magnification of  $V_{resp}$  due to the multi-direction excitation, it seems that one-direction horizontal seismic motion should be enough to assess seismic stability of the metal cask attached to a transfer pallet.



(Type-A) (Type-B)  
Fig.12 Relationship between  $V_{WES}$  and  $V_{resp}$

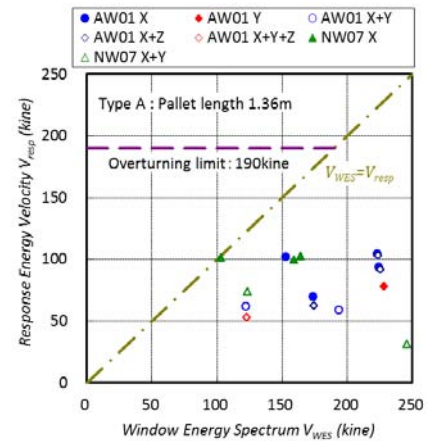


Fig.13 Multi-axis excitation test results for Type-A

## CONCLUSIONS

In Japan, in order to assure the seismic stability of the metal cask during the strong seismic motions, a metal cask will be attached to a transfer pallet. As a metal cask will be operated vertically in the free-standing condition on the floor pad in the cask storage facility, the prevention of the overturning of the cask due to the very severe seismic load is one of the technical key issues not to damage its safety functions. In order to clarify the seismic characteristics of the metal cask attached to a transfer pallet, the experimental studies are performed by the excitation tests with a scale model cask using large-scale shaking table test equipment. According to the test results, it is found that the proposed window energy spectrum would be practical and conservative design parameter to estimate the possibility of the overturning of the metal cask attached to a transfer pallet.

## REFERENCES

- [1] KAWAGUCHI, S., et al., Stability Evaluation of Metal Cask Attached to a Transfer Pallet during Long-Period Seismic Motions, J. of JSCE, Ser.A1 (SE/EE), Vol.68, No.2, 271-286, 2012. (in Japanese)
- [2] SHIRAI, K., et al., Experimental Studies of Free-Standing Spent Fuel Storage Cask subjected to Strong Earthquake, SMiRT17, K470, Prague, Czech, Republic, Aug., 2003.
- [3] AKIYAMA, H., et al., Estimate of Overturning of Rigid Bodies with Energy Spectrum, J. Struct. Constr. Eng., AIJ, No.488, 49-55, Oct., 1996. (in Japanese)
- [4] AKIYAMA, H., et al., Relationship between Energy Spectra and Velocity Response Spectra, J. Struct. Constr. Eng., AIJ, No.608, 37-43, Oct., 2006. (in Japanese)